Intelligent Underwater Object Detection and Image Restoration for Autonomous Underwater Vehicles

Sheezan Fayaz, Shabir A. Parah, *Member*, *IEEE*, G. J. Qureshi, Jaime Lloret, *Senior Member*, *IEEE*, Javier Del Ser, *Senior Member*, *IEEE*, Khan Muhammad, *Senior Member*, *IEEE*

***Abstract*—Unmanned Underwater Vehicles (UUVs) have been reliable and economical technological solutions to perform undersea monitoring tasks in comparison to manned vehicles. However, in many situations, UUV is unable to fulfill complex undersea research tasks since target objects appear distorted due to light absorption and scattering. Besides, ocean surveying undergoes severe power requirements compared to terrestrial systems because of battery-driven low-storage vehicles like Unmanned Underwater Vehicles (UUVs). Therefore, limited power supply, motion resistance of water medium, and distorted target object appearance can delay the mission and reduce the efficiency of UUV in their underwater operations. Considering the resource-constrained undersea monitoring setup, we propose an intelligent two-stage framework for expeditious monitoring of underwater scenes. First, an effective deep neural network is employed for underwater object/region of interest (ROI) detection. Then the detected ROI is restored using an efficient restoration method, thereby improving the visual quality of the degraded images and aiding the navigating and monitoring tasks of UUVs. Our method has been objectively and subjectively assessed using 9 evaluation metrics and our key results reveal mAP of 94.35% and an Underwater Color Image Quality Evaluation (UCIQE) score of 3.09, surpassing state-of-the-art methods for object detection. Furthermore, the execution time of 0.550 secs is required for object detection and dehazing, making this proposal suitable for UUVs to perform automatic undersea object detection and dehazing within operational running requirements.**

***Index Terms*—**Dark Channel, Deep Learning, Object Detection, Image Restoration, Unmanned Underwater Vehicles.

I. INTRODUCTION

THE UUV is receiving huge attention for applications not just limited to scientific undersea exploration [1],[2] but also, for applications, like military, fishing, hull inspection, deep-sea survey, undersea construction and rescue, monitoring seafood, pipeline detection and seabed mapping [3]. UUVs self- propelled and unmanned intelligent components employ automatic controllers and visual sensors [4]. In particular, Optical Subaquatic Vehicles (OSVs) having optical sensors providing better scene details of an undersea environment, are extensively employed to achieve complex and dynamic missions. The overall architecture of UUV and challenges of underwater imaging are discussed in the following section.

Manuscript received April 7, 2023; revised August 15, 2023; accepted September 2, 2023; published: XXXX. This work was supported by the Department of Electronics and Instrumentation Technology, under Grant DST/TDT/SHRI-33/2018, funded by the Indian Government under Science and Heritage Research Initiative (SHRI) scheme. J. Del Ser acknowledges funding support from the Basque Government through ELKARTEK and EMAITEK funds, as well as the Consolidated Research Group MATHMODE (IT1456–22). (Corresponding authors: Khan Muhammad and Shabir A.Parah).

Sheezan Fayaz, Shabir A. Parah, and G. J. Qureshi are with the Department of Electronics and IT, University of Kashmir, Srinagar, India and with the Higher Education Department, Government of Jammu and Kashmir, India (e-mail: shezan_fayaz@yahoo.com, shabireltr@gmail.com).

Jaime Lloret is with the Instituto de Investigación para la Gestión Integrada de Zonas Costeras (IGIC), Universitat Politécnica de Valencia, Valencia, Spain (e-mail: jlloret@dcom.upv.es).

Javier Del Ser is with TECNALIA, Basque Research & Technology Alliance (BRTA), 48160 Derio, Spain, and also with the Department of Communications Engineering, University of the Basque Country (UPV/EHU), 48013 Bilbao, Spain (e-mail: javier.delser@tecnalia.com).

Khan Muhammad is with the Visual Analytics for Knowledge Laboratory (VIS2KNOW Lab), Department of Applied Artificial Intelligence, School of Convergence, College of Computing and Informatics, Sungkyunkwan University, Seoul 03063, Republic of Korea (e-mail: khan.muhammad@ieee.org).

II. BACKGROUND AND RELATED WORK

i) Overview of generic UUV

Architectural solutions suited for UUV pose high processing challenges, exacerbated by their limited power availability. Following are the nodes involved in a typical UUV architecture, which are described to illustrate its working procedure:

- **Vehicle Head Box (Node 1)**: it governs the vehicle movement, camera power, illumination, pitch, yaw, and roll (tilt survey).
- **Doppler velocity logger - DVL (Node 2):** it performs data acquisition.
- **GPS and Engine Management (Node 3):** it implements several tasks such as reading GPS data, managing engine, and controlling dive, propulsion, and rudder.
- **Sensor Reading (Node 4):** undersea instrumentation sensor analysis and the management of their energy requirements.
- **Vehicle Controller (Master Node)**: it collects data to be processed from every node, and generates commands accordingly. The controller connects the network to the Ethernet.

Fig. 1 gives an overview of UUV architecture employed for underwater monitoring tasks.

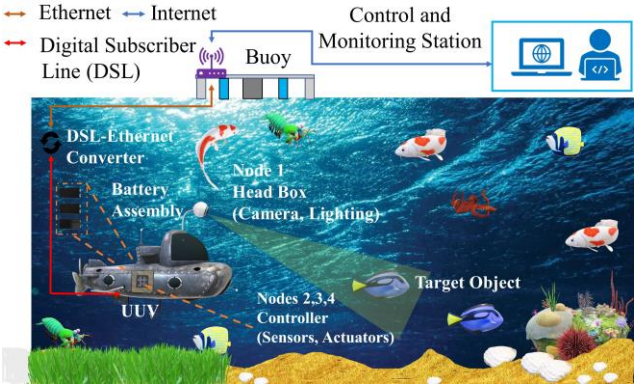

Fig. 1. Overview of Undersea UUV

ii) Challenges posed by underwater imaging

The UUVs automatic control mechanism obtains multi-scale visual data from undersea environment through optical sensors. It also employs automatic control technique to take the decision to avoid undersea obstacles, thus, rendering the task of both dynamic decisiveness and optical navigation. However, navigating battery-driven low storage UUVs in complex undersea environment immensely hinders the undersea monitoring tasks. The challenges are posed mainly by dispersion and absorption of light which degrades quality of subaqueous pictures showing reduced level of contrast with color distortion. This results in obtaining the distorted visual data by the UUVs from the complex undersea environment, impeding its decisive capability of avoiding obstacles. Besides, the availability of limited resources put forth a constriction and may result in delaying the mission. Therefore, the efficiency of UUVs has been limited by the challenge of obtaining undistorted, haze-free underwater images for effective monitoring of the scenes via less complex frameworks.

In underwater imaging, three types of light radiation fall on the camera: direct transmission i.e., the light radiation directly reflected from the target sub-aquatic object; forward-scattering radiation that originates when light rays collide with tiny, suspended particles, thereby scattering before reaching the aperture of the camera; and background-scattering that is light energy from the atmospheric light which gets reflected by the water particles. Thus, an undersea picture is mathematically given by a sum of back-dispersing, forward-dispersing, and uninterrupted transmission.

$$\mathrm{E_t(u,v)} = \mathrm{E_d(u,v)} + \mathrm{E_f(u,v)} + \mathrm{E_b(u,v)} \qquad (1)$$

Where *(u,v)* indicates the coordinates of a pel; $E_t(u,v)$ denotes the total light energy falling on the camera. $E_f(u,v)$, $E_d(u,v)$, and $E_b(u,v)$ indicate the forward-dispersing, uninterrupted transmission, and back-dispersing components, respectively. If space from sub-aquatic target to camera aperture is less, then the forward-dispersed light may be forsaken and just $E_d(u,v)$ and $E_b(u,v)$ are considered.

To restore an underwater image, the mathematical model that is extensively employed for misty degraded images in computer vision is.

$$\mathrm{I(e)} = \mathrm{J(e)t}(e) + \mathrm{A}\big(1 - \mathrm{t(e)}\big) \qquad (2)$$

I(e) indicates the input pel at point e, *J(e)* represents the haze-free image, *t* represents transmission map that is the light that falls on the aperture of camera without dispersing, and *A* denotes the atmospheric light. Aforementioned expression is known as Image Formation Model (IFM). The proposed method employs Eq. (2) for undersea image restoration. The image restoration algorithms aim at computing true or dehazed scene radiance which greatly relies on the computation of unknown variables such as atmospheric light *A* and transmission map *t(e)*.

iii) Related work

To address the issues of resource constraints and considering the ill-posed problems of underwater imaging, ocean engineers have come up with neural networks that are employed in many disciplines for solving complex automatic problems. Neural networks are employed to process an immense number of images and involve specialized systems to reduce operational speed and storage requirements [5]. Computationally complex tasks like subaquatic image monitoring, processing, subaquatic object detection, and recognition can be outsourced to a specialized Deep Neural Network (DNN) for faster execution. Thus, a hybrid method involving a neural network-based underwater object detection and effective underwater image restoration can pave a way for efficient real-time applications in resource-constrained UUV setup. A thorough literature survey indicates that efficient neural computing-based techniques are relatively less employed in UUV for the precise navigation, exploration of marine life, instantaneous monitoring of the marine ecosystem, and execution of other underwater research tasks that are substantial. It is due to the fact that in UUV frameworks, expeditious monitoring is a challenging task. Although, due to the advent of PUVs (Piolet-less Undersea Vehicles), AUVs (Automatic Undersea Vehicles), digital cameras etc., the availability of underwater imagery has exponentially increased lately. However, the power capacity of the battery used in AUV is a limiting factor keeping the navigating and monitoring operations limited in duration and range, usually as little as 24 hrs. The cruising speed of deep-sea exploration vehicles is 3 kts (1.543m/s) and the average speed of deep tow is 2knts (1.028m/s). The adversity surges by the additional light scattering and light absorption phenomenon that interferes with efficient and expeditious underwater imaging.

For automatic and instantaneous monitoring of underwater images and solving undersea issues, deep learning which is SOTA field of ML (Machine Learning) presents unparalleled potential opportunities. Till now low-level manually designed features have been exploited in earlier conventional methods of classification. Also, Support Vector Machine (SVM), Principal Component Analysis (PCA), Linear Discriminant Analysis (LDA), and other conventional machine learning approaches are quickly saturated if the training dataset increases. As the availability of digital images is greatly increasing with time, there is a requirement for improved access techniques for retrieving images from a massive image database. Deep Neural Networks (DNNs) enable researchers to resolve several underwater issues such as protecting undersea ecological conditions, sub-aquatic disaster reduction and prevention, emergency rescue, detecting a sub-aquatic target, its recognition, and tracking. DNNs can be employed for underwater systems such as classifying and recognizing underwater data (CNN) [6], reconstructing underwater data (CNN) [7], and predicting underwater information (RNN: Recurrent Neural Network), (CNN) [8]. In this line of research, Libao et al., [9] proposed a new approach for saliency analysis and extraction of Region of Interest (ROI) for remote sensing pictures. The algorithm consists of intra-spectrum information distribution computation for pictures that are multi-spectral and a local-global contrast analysis for panchromatic pictures. For pictures, audios, texts, etc., to be meaningful, DNNs perform the transformation of input data through several layers than the networks that employ shallow learning [10]. Each layer is used to transform the signal with the help of a computing unit called

neuron that grasps parameters by training. The aforementioned discussion presents a lot of algorithms that are primarily governed by neural networks, however, efficient DNNs that have less computational complexity have been hardly used in UUVs for object spotting and its classification. Also, at one end many software-based services have greatly increased, on the other end, for the quality services, the expectations are significantly rising. To meet the requirements, we attempt to make use of an efficient DNN that employs the latest version of the You Only Look Once Version 8 (YOLOV8) object detection framework. We have also performed the ROI detection experiment using YOLOV4. In the proposed technique, YOLOV8 is responsible for ROI detection and extraction reducing the size of an image and hence resource requirements. Subsequently, the extracted ROIs are passed over to the novel and precise dehazing algorithm to further enhance sea life monitoring performed via autonomous vehicles. We aim to detect ROI in an image and yield high-quality images in a reduced amount of time to aid the UUV navigation and decisiveness to avoid obstacles.

We made several major contributions to the underwater monitoring via UUV network which are summarized as follows:

1. The proposed framework is a two-stage system for addressing momentous issues of poor quality in underwater images and resource constraints in UUVs.
2. Our proposed method automatically performs the region of interest (ROI) detection and extraction, ensuring higher operational speed by using an efficient neural computing mechanism. DNN has been employed in this stage due to its fast inference time.
3. The detected ROI having reduced size and only useful data is restored using an efficient and precise restoration method, thereby improving the visual quality of the degraded underwater images and aiding the subaquatic monitoring process performed by UUVs in undersea environments.
4. The redundant data in the underwater images is eradicated to reduce their sizes, hence reducing processing time and other resources like bandwidth, transmission power, and storage required in UUV setup for full coverage communication to survey underwater environments. The proposal is evaluated both subjectively and objectively (using 9 evaluation scores) and the results surpass SOTA.

Rest sections of the manuscript are as follows: Background of our technique comes under Section II. Our technique has been discussed in detail in Section III. Section IV highlights performance evaluation based on comparison of our method with SOTA. Section V concludes proposed work and puts forth future work.

III. PROPOSED METHODOLOGY

Considering the limitations ocean engineers come across while dealing with the unmanned vehicles, the proposed framework employs efficient DNN to detect and extract underwater ROIs. The framework is a two-stage model and aims to efficiently detect, extract ROIs, and restore underwater blur ROIs keeping in view the UUV navigation in complex environment and its resource constraints. The famous undersea UUV system employs battery-driven device. It is less expensive than conventional vessels; however, the power capacity of the battery is a limiting factor making the undersea surveys limited in range and duration. Thus, in the proposed framework the trivial data in the undersea images is eliminated which reduces image sizes, thereby reducing processing time, bandwidth requirement, transmit power, and storage like resources required for effective underwater surveillance.

The first stage performs speedy ROI detection in degraded undersea images. For this stage, we have employed both YOLOV8 and YOLOV4 to compare the performance of both versions for efficient ROI detection. YOLOV8 is a deep neural network that enables fast target spotting/detection. RCNN (Region-based convolutional neural network) first extracts many region proposals from the input image. Then a CNN network is used to perform forward propagation on every extracted region proposal to draw out features. Subsequently, features from each region proposal are utilized to perform prediction of the class and the boundary box for that region proposal. On the contrary, the YOLOV8 takes just single forward propagation through DNN to detect targets. It indicates, in only single go of the network, predictions over the entire underwater picture are performed. At the same time, the prediction process of bounding boxes and probabilities associated with varied classes is performed.

Subaqueous dataset employed for training and testing of the YOLO (V4 and V8) model has been curated and it consists of some substantial underwater species and objects i.e., fish, human divers, and submarines.

The second stage of the proposed network performs the restoration of degraded underwater ROIs that have been detected and extracted by the first stage. This stage employs the restoration algorithm which tends to dehaze the underwater images with fewer inaccuracies because of the less erroneous prior information. UDCP is an algorithm that is prior-driven and can result in massive errors in estimation if prior information like medium transmission and air light or atmospheric light is erroneous. Thus, a need of increasing the precision in such estimations comes to light for producing output undersea pictures with pleasing appearance within less time. For UDCP - Undersea Dark Channel Prior, brightest pel in undersea picture is often considered atmospheric light. This prior data is invalid and incapable of yielding good results if an object in a picture is brighter compared to atmospheric light. Moreover, the precision in TM (Transmission Map) estimation relies on the computation accuracy of BL (Background Light). Previous prior driven algorithms for undersea image restoration including DCP and UDCP calculate the TM of just single channel and assume the medium transmissions of the rest of the color channels are the same which results in distorted textures, block artifacts, plus halo artifacts over the recovered undersea picture. Such distortions creep into the process because the medium transmission of the three channels is not always the same in a local patch. Therefore, to address these issues, we have employed the algorithm which estimates the TMs of each of the three colors i.e., RGB. To decrease the complication in proposed algorithm, we compute transmission map of the blue channel from the mathematical relation of a misty picture representation, then estimate TMs of rest of the GB colors using the arithmetic relation of medium TMs of the green-red channels with the blue channel. Thus, our technique break

downs the issue to a single-color TM computation, nevertheless, computes the TMs of all channels with no compromise on picture quality.

Eq. (2) indicates misty picture representation. Just to not have confusions, for proposed scheme, the undersea dark color channel calculated via our algorithm is indicated by J_{MUWDCP}. The dark channel is calculated using GB channels. The true scene of particular channel computed by our scheme is represented by J_{mc}. Therefore,

$$\mathrm{J_{MWUDCP}} = \min_{\mathrm{c\epsilon g,b}}\left(\min_{\mathrm{y\epsilon\pi}(e)} \mathrm{J_{mc}}\,(\mathrm{y})\right) \quad (3)$$

$$\mathrm{J_{MUWDCP}} \to 0$$

Min filters are applied to the misty picture expression, then considering the idea of proposed scheme,

$$\min_{\mathrm{c\epsilon g,b}}\left(\min_{\mathrm{y\epsilon\pi(e)}} \mathrm{I}_c(y)\right) = \min_{\mathrm{c\epsilon g,b}}\left(\min_{\mathrm{y\epsilon\pi(e)}} (\mathrm{J}_{mc}(y)\mathrm{t}(e))+_{\mathrm{c\epsilon r,g,b}}(\mathrm{A}_{mc}(1 - \mathrm{t(e)})\right) \quad (4)$$

A_{mc} denotes the global atmospheric light. On normalizing the Eq. (4) with respect to A_{mc}, we have,

$$\left(\frac{\min_{\mathrm{C\epsilon b,g}}(\min_{\mathrm{Y\epsilon\pi}(e)}(\mathrm{I_C(y)}))}{(\mathrm{c\epsilon r,g,b}\mathrm{A_{mc}})}\right) = \mathrm{t(e)}\left(\frac{\min_{\mathrm{c\epsilon b,g}}(\min_{\mathrm{Y\epsilon\pi(e)}}\mathrm{J_{mc}(y)})}{(\mathrm{c\epsilon r,g,b}\mathrm{A_{mc}})}\right)+1 - \mathrm{t(e)} \quad (5)$$

$\mathrm{A_{mc}}$ is estimated using RGB color channels of the deteriorated undersea image. To robustly calculate the BL, our scheme has used a statistical approach on chosen highest intensity pels of deteriorated undersea picture. A mode approach is proposed for calculating global airlight using hazy undersea picture. Th technique is implemented on the RGB-colors because light radiation can be computed separately in each color channel. First of all, pels of the window π which has center at e of deteriorated undersea image are chosen, then organized in decreasing order of pel values. Subsequently, among those pels, about one percent of the pels with the highest brightness are selected from each color channel, then the pel with maximum repetition i.e., highest probability pel gets selected as airlight. Thus, undersea channel that contains dark pels estimated via GB colors, also pel showing maximum repeated occurrence in highest intensity pels i.e., airlight are placed in Eq. (5), and the expression for medium TM is obtained as,

$$\mathrm{t}_{bl}(\mathrm{e}) = 1 - \left(\frac{\min_{\mathrm{C\epsilon b,g}}(\min_{\mathrm{Y\epsilon\pi(e)}}\mathrm{I_C(y)})}{(\mathrm{c\epsilon r,g,b}\mathrm{A_{mc}})}\right) \quad (6)$$

The medium transmission map computed using Eq. (6) has been considered as TM of channel blue (B). This supposition is made on the certitude that channel blue has the shortest wavelength out of RGB channels, thus, it travels most underwater. Based upon this fact, TM at e is indicated as $t_{bl}(e)$ which is TM of channel blue. According to Schechner et al. [11], TM at spot x i.e., $t_c(e)$ is shown as:

$$\mathrm{t_c(e)} = \mathrm{e}^{-\eta_c \mathrm{d(x)}} \quad (7)$$

$d(x)$ gives the camera-object distance, η indicates attenuation factor that can be computed via a summation of absorption factor a and scattering factor b, thus, $\eta = a + b$. Moreover, Li et al. [12] proposed that in underwater conditions, the ratios of the attenuation coefficients of different colors can be given as:

$$\frac{\eta_\mathrm{r}}{\eta_\mathrm{b}} = \frac{(-0.00113\lambda_\mathrm{r} + 1.62517)\mathrm{A_b}}{(-0.00113\lambda_\mathrm{b} + 1.62517)\mathrm{A_r}} \quad (8)$$

$$\frac{\eta_\mathrm{g}}{\eta_\mathrm{b}} = \frac{(-0.00113\lambda_\mathrm{g} + 1.62517)\mathrm{A_b}}{(-0.00113\lambda_\mathrm{b} + 1.62517)\mathrm{A_g}} \quad (9)$$

Where $\frac{\eta_g}{\eta_b}$ and $\frac{\eta_r}{\eta_b}$ are the total attenuation factors of GB and RB channels, wavelengths of various colors are denoted by λ_c. Generally, λ_g, λ_r, and λ_b are around 550nm, 700nm, and 450nm, respectively. Hence, the TMs of the rest of the RG-color channels can be estimated from the equations shown below:

$$\mathrm{t_r(e)} = \left(\mathrm{t_b}(e)\right)^{\frac{\eta_\mathrm{r}}{\eta_\mathrm{b}}} \quad (10)$$

$$\mathrm{t_g}(e) = \left(\mathrm{t_b}(e)\right)^{\frac{\eta_\mathrm{g}}{\eta_\mathrm{b}}} \quad (11)$$

To further eradicate the distortions in recovered undersea picture, medium TM is enhanced with a guidance filter [13]. Fig. 2 highlights the process flow of our method. Besides, the outline of the proposed method is given in Algorithm 1.

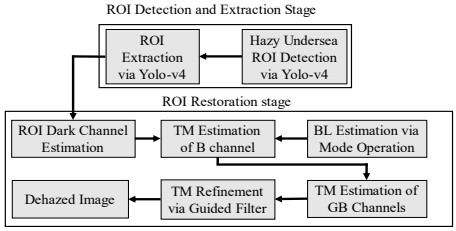

Fig. 2. General process flow of our method

Algorithm 1: Steps Involved in Proposed Method

1. Given input I(e)
2. Detect and Extract ROI Fish, Diver, Submarine
3. Fish = 1000, Diver = 1000, Submarine = 1000
   Total number of images = 3000
   Training images = 2400
   Testing images = 600
4. Solve the following sub-problems:
   (i) Compute J_{MUWDCP} from (3)
   (ii) Compute A_{mc} using mode operation.
   (iii) Compute $t_b(e)$, $t_g(e)$, and $t_r(e)$ via (6) – (11).
   (iv) Refine medium TM.
5. Extract Output J(e)
6. Return Dehazed ROI

IV. RESULTS AND DISCUSSION

This part of manuscript has been divided into four sections: Firstly, object detection method is evaluated, and the results are presented in Section IV (A). Next, the image restoration method is evaluated from different aspects and is compared with SOTA as given in Section IV (B). In Section IV (C), an overall comparative study of our proposal with SOTA is presented using both subjective and objective evaluation. Finally, Section IV (D) highlights the benefits of the proposed method in undersea monitoring tasks, supporting unmanned vehicle framework.

A. Results by Our Object Detection Method

Experiment for underwater object detection and ROI extraction has been performed and our model has been trained using GPU NVIDIA Tesla K80. The undersea detection has

been performed via YOLOV4 and YOLOV8. We select the so-called medium-sized version of YOLOV8 (i.e., YOLOv8m).

In the object detection process, Precision, Recall, and Mean Average Precision are often employed for checking the accuracy of the algorithm. The model used for comparison has learnt via training performed using degraded undersea picture dataset comprising submarines, divers, and fish. These three kinds of underwater objects are the vital resources of the underwater world and summarize the subaqueous target spotting operation for rest of subaqueous targets. We have employed 3000 curated undersea images; out of these 2400 images have been used for training the algorithm and 600 images have been used for testing and the batch size is 128. The framework performs the underwater object detection with a Mean Average Precision (mAP) = 94.6%, Recall = 90.6%, and average Intersection over Union (IoU) = 79.1%. Besides, YOLOV8 performs the ROI detection with mAP = 94.35% and precision = 94.60%, in approximately 0.028 ms enabling an instantaneous underwater ROI detection and extraction, which in turn results in speedy dehazing and restoration of blurred underwater images.

Table I highlights precision and mAP values of Fast RCNN, Faster RCNN, and YOLOV3 for images from "Underwater Robot Picking Contest" compared with the precision and mAP scores of our method employing YOLOV4 and YOLOV8 for curated underwater submarines, divers, and fish.

Recall, mAP, and speed i.e., Frames per Second (FPS) are used to compare the accuracy and speed of YOLO(V4 and V8) based proposed method, Faster RCNN, and YOLOV3. The obtained results are shown in Table II. The dataset from popular site URPC (UNDERSEA ROBOT PICKING CONTEST) is converted to the VOC2007 format for comparison.

TABLE I
COMPARISON OF OUR METHOD TRAINED ON UNDERSEA FISH, SUBMARINE, AND DIVER WITH FAMOUS DNNS

Parameters		Networks					
		Fast RCNN	Faster RCNN	YOLO V3	YOLOV4		YOLOV8
mAP (%)		27.26	27.53	35.43	94.35		94.60
Precision %	Sea-Cucumber	30.13	30.18	37.14	Fish, Sub-marine and Diver	94	94.3
	Sea Urchin	26.79	27.29	35.42			
	Scallop	24.87	25.13	33.74			

TABLE II
PERFORMANCE COMPARISON OF OUR METHOD WITH OTHER DNNS

Networks	mAP (%)	Recall (%)	FPS
Faster RCNN	69.7	75.6	8
YOLOV3	76.1	89.5	20
YOLOV4	94.35	90	31
YOLOV8	94.6	90.6	30

Furthermore, a comparison is also made with Xu and Matzner [14] that have employed three different datasets to compute mAP values for their algorithm. Table III indicates the mAP values yielded by Xu and Matzner and our model trained on degraded undersea images.

It can be seen from the results that our method performs better and is more efficient. Besides, there is not considerable difference seen in ROI detection time and precision for YOLO V8 and V4. Since the proposed algorithm is a two-stage network, the performance evaluation of the second stage is carried out in the following Section IV (B).

TABLE III
COMPARISON OF MAP VALUES USING DIFFERENT DATASETS

Techniques	Datasets	mAP (%)
Xu and Matzner [14]	Wells Dam	55.75
	Voith Hydro	54.74
	Igiugig	45.07
Our method	Curated	94.6

The second stage consists of an underwater image restoration algorithm that provides more accuracy in estimating the prior data. Hence, the algorithm greatly improves the quality of images and produces subaqueous pictures with visually pleasing appearance.

B. Performance Evaluation of Restoration Method

The ocular artifacts result in perversions having non-linear characteristics and may badly affect visual operations and subaqueous operations for science related and ocean survey works e.g., tracking, monitoring subaqueous world, classifying picture objects etc.

i) Comparing Proposed Method Airlight Computation with SOTA Techniques

Several approaches used to estimate the TM rely also on calculated BL/Airlight. Therefore, various subaqueous picture restoration algorithms require to get compared in terms of BL estimation. Addressing this issue, this section is included for comparing the various algorithms employed for BL computation. For comparing BL estimated by different prior-driven restoration methods, we have selected an undersea image, as shown in Fig 3.

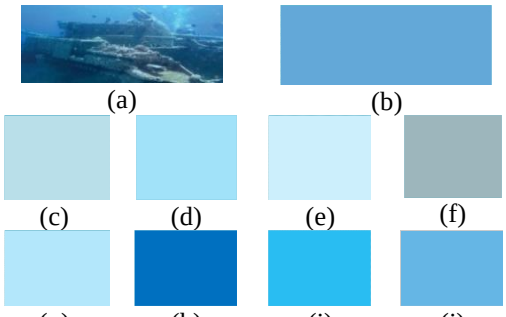

Fig. 3. (a) Misty subaqueous Image, (b) Ground Truth BL, (c) UDCP [15], (d) DCP [16], (e) DCP [17], (f) DCP [18], (g) DCP+MIP [19], (h) MIP [20], (i) IBLA [21], and (j) Proposed Method.

Ground truth BL of the undersea test picture as shown in Fig 3 (b), has been acquired via around ten-fifteen person's feedbacks based upon concept to select distant subaqueous target from capturing device and radiation for backdrop illumination. Fig. 3 (c) to (i) show results of various popular picture dehazing algorithms. UDCP execution in Fig. 3 (c) is like DCP. Output of DCP [16] is given in Fig. 3 (d), indicating airlight calculation using the concept of Dark channel prior. Calculated airlights of DCP [17], DCP [18], DCP +Maximum Intensity Prior (MIP) [19], MIP [20], Image Blurriness and Light Absorption (IBLA) [21] are shown in Fig. 3 (e) to (i). Survey [22] reveal methods to calculate airlight through DCP

scheme do not recklessly choose pel with the highest brightness as airlight, but ignores visual imaging characteristics of the undersea conditions depicting substantial variations in R and BG colors, hindering DCP from estimating airlight. Also, Fig. 3 (j) indicates result of our technique.

ii) Comparing Medium TM Computation with Well-known SOTA Techniques

In various methods used to calculate medium TM, it has been observed, nearer an undersea image is to aperture, greater is medium TM value, and seems whitish. In contrast, farther the undersea pictures will be, the dimmer will be their medium TMs. Fig. 4 (a) indicates the hazy undersea picture employed to estimate TM. For the high visual quality representation of TM, a guided filter [13] is employed for TM refinement. Fig. 4 (b) shows the TM result of the UDCP. Fig. 4 (c) and (d) depict DCP's estimated TM, which is not precise. The difficulty comes into being because of less accurate calculation of airlight. DCP chooses maximum valued pel as airlight, that may be an inherently bright undersea object or can be illuminated point. Taking this fact into consideration, airlight may lead to erroneous scene depth-map and can produce erroneous medium TMs of scenes. Fig. 4 (e) and (f) represent medium TMs computed using renowned prior-based methods like MIP, IBLA, and Fig. 4 (g) shows results of our technique. The figure reveals the proposed technique performs better as it generates clearer transmission maps.

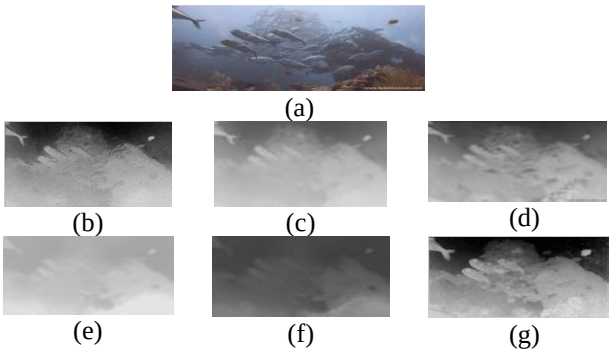

Fig. 4. (a) Misty Subaqueous Image [13] (b) TM Estimated Using UDCP [15], (c) TM Estimated Using DCP [16], (d) TM Estimated Using DCP [23], (e) TM Estimated Using MIP [20], (f) TM Estimated Using IBLA [21], and (g) TM Estimated Using Proposed Method.

C. Overall Performance Evaluation

The proposed framework is a combination of a deep learning-based object detection algorithm and a prior-based image restoration algorithm. Our framework involves two networks to accomplish the task of instantaneous and effective dehazing considering the problem of resource constraints. Thus, in this section, we have presented the experimental outputs of overall network. For evaluating the undersea image quality, both quality plus quantity-based methods have been employed for comparing DCP [24], UDCP [15], and proposed method. To measure the quality level of an undersea image, Image quality assessment (IQA) has been employed, and it is categorized into Objective Evaluation (OE) and Subjective Evaluation (SE).

(1) Objective Evaluation (OE)

Due to the unavailability of ground-truth images, we have chosen quality metrics like Entropy, UIConM, UIQM [25], and UCIQE [26] to assess and rate the nonreference pictures. Besides, the time analysis of the algorithm has also been performed.

Table IV tabulates the values of UCIQE, Entropy, and UIQM of undersea pictures with dimensions equal to 400 × 600 recovered by DCP [17], UDCP [27], Image Blurring and Light Absorption (IBLA) Prior [21], UDCP (TEoUI- TM Estimation in Undersea Single Images) [15], Maximum Intensity Prior (MIP) [20], Underwater Light Attenuation Prior (ULAP) [22], and the proposed method.

TABLE IV
COMPARISON OF SOTA WITH OUR ALGORITHM

METHOD	ENTROPY	UCIQE	UIQM
UDCP	6.48	0.55	2.51
IBLA	6.84	0.59	1.47
MIP	6.54	0.52	0.78
DCP	6.39	0.50	0.16
UDCP (TEoUI)	6.99	0.58	2.84
ULAP	6.75	0.58	3.70
Proposed Method	**7.25**	**3.09**	**8.97**

We have also computed the UIQM and UIConM scores of hazy and dehazed 400×400 images. Fig. 5 highlights the enhancement of UIQM and UIConM values by the proposed method.

UIConM (Dreg.) and UIConM (Res.) represent the UIConM values of degraded and restored undersea images, respectively. Similarly, UIQM (Dreg.) and UIQM (Res.) represent the UIQM values of degraded and restored undersea images, respectively.

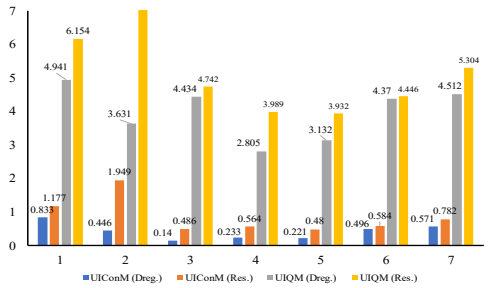

Fig. 5. UIConM and UIQM Values of Degraded and Restored Underwater Images

From the bar chart, it is seen that the proposed algorithm increases the UIConM and UIQM scores, thus improving the appearance of a subaqueous picture. Average values of UIConM and UIQM on seven 400×400 restored underwater images are 0.860 and 5.364, respectively. Furthermore, for the time analysis, we have compared the proposed algorithm with the popular schemes like DCP and UDCP in terms of time in table V.

TABLE V
TIME COMPARISON OF SOME ALGORITHMS WITH PROPOSED ALGORITHM

Serial No.	Algorithms	Time (secs)
1.	DCP [24]	2.121
2.	UDCP [15]	3.845
3.	Proposed	0.55003

Also, the time taken to restore detected ROIs by UDCP, and our technique is highlighted in Fig. 6. In addition, our scheme is compared to latest techniques employed to recover and

enhance subaqueous picture such as J. Yuan et al., [28], 2022; Wang et al. [29], 2017; Peng et al., [21], 2017; Song et al., [22], 2018; Pan et al., [30]; 2019, and Zhuang et al., [31]; 2020. The performance comparison is carried out based on UIQM depicted by Table VI and subaqueous picture dimension is 512 × 512.

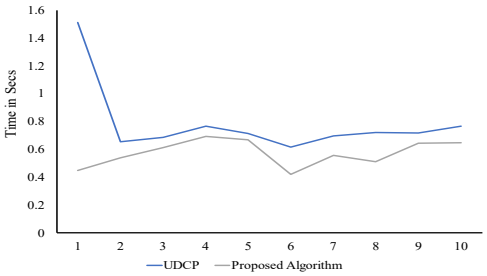

Fig. 6. Time analysis of the proposed algorithm and UDCP

TABLE VI
COMPARISON OF PROPOSED METHOD WITH SOTA

S.No.	Techniques, Year	UIQM
1.	J. Yuan et al. [28], 2022	4.869
2.	Zhuang et al. [31], 2020	4.93
3.	Pan et al. [30], 2019	4.08
4.	Song et al. [22], 2018	3.98
5.	Wang et al. [29], 2017	4.19
6.	Peng et al. [21], 2017	4.07
7.	Peng et al. - Histogram Equalization [21], 2017	4.89
8.	Our Method, 2023	**6.274**

Also, using UCIQE scores, latest subaqueous picture dehazing techniques namely, Peng et al. 2017 [21], Pan et al. 2019 [30], and Hou et al. 2020 [32] are compared with the proposed algorithm. From Table VII, it is highlighted average UCIQE of every comparative method is smaller than our mechanism. Mostly, the UCIQE of our algorithm has been higher than 1. The high UCIQE means the dehazed undersea images of the proposed scheme show fine balance in saturation, degree of contrast, and degree of chroma.

TABLE VII
UCIQE VALUES OF PROPOSED AND SOME RECENT ALGORITHMS

S. No.	Techniques	UCIQE
1.	Peng et al. [21]	3.00
2.	Peng et al. + Hist [21]	3.767
3.	Pan et al. [30]	0.605
4.	Hou et al. [32]	0.6003
5.	Proposed Method	**3.815**

TABLE VIII
TIME COMPARISON OF PROPOSED ALGORITHM WITH CNN BASED ALGORITHM

No.	Algorithms	Time (secs)
1.	TEBCF [28]	7.75
2.	ECNN [33]	30
3.	Proposed Method	**0.56**

Besides, a time comparison of our technique and latest subaqueous picture recognition scheme and texture-based dehazing scheme by Saifuddin Saif [33] in 2021 and J. Yuan et al. [28] in 2022, respectively is shown in Table VIII. The algorithm proposed by Saif [33] is based on enhanced convolutional neural network (ECNN) [33].

(2) Subjective Evaluation (SE)

ROIs detected and restored using proposed scheme have been compared to the restored ROIs of UDCP and DCP. Fig. 7 shows the overall image quality of restored ROIs of various prior-based techniques. It is concluded considering underwater images indicated in Fig. 7 that our method recovers undersea pictures showing improved visual quality than UDCP. Results produced by the UDCP seem to be unnatural and oversaturated.

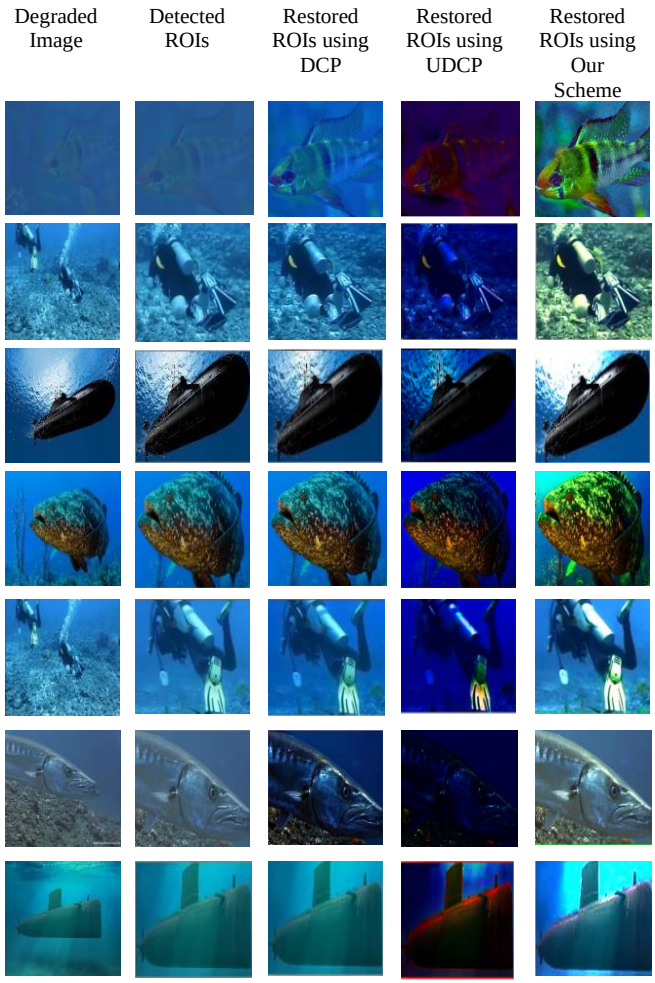

Fig. 7. Comparison of Proposed Algorithm with UDCP [13] and DCP [22].

From the first and fourth images of the fifth column, it is clear that our scheme enhances the fine details of the image and restores the intricate information in the image as well. Besides, proposed method also protects the natural look of the sub-aquatic picture, producing high-quality outputs that are not extremely saturated.

Several popular state-of-the-art algorithms attempt to perform underwater image restoration; however, these algorithms are either computationally complex hence not suitable for UUV setup or estimate less accurate prior data. DCP and UDCP do not propose accurate prior data i.e., the transmission map and the atmospheric light on which the quality of restored underwater image relies. Addressing these issues, the proposed method aims to increase the fidelity of the estimated prior information, reduce the computational time, and resource requirements conforming to the UUV requirement guidelines.

The overall operational time taken by our technique goes hand in hand with the cruising speed of unmanned underwater vehicles. Also, pertinent to mention here that YOLOV8 and YOLOV4 models have been trained on highly degraded images of underwater scenes, nevertheless, the algorithm shows better accuracy with speedy detection supporting the main paradigm of unmanned monitoring.

D. Benefits of the Proposed Method in Unmanned Underwater Vehicle Monitoring Network

Autonomous monitoring tasks are often constrained by the energy and computation limitations of underwater devices like UUVs, underwater sensors etc. [34], [35]. The transmission distance in undersea environments is more than the terrestrial transmission distance leading to huge demand of resources like transmit power, bandwidth, etc. [36], [37], [38]. Besides, degraded and less visible underwater images cause an additional surge in the issue of resource scarcity and limit the effective monitoring and navigation across oceans via UUV setup. Thus, the proposed algorithm aims at detecting and improving the visual quality of substantial underwater objects at the cost of least resource consumption. The algorithm performs instantaneous and automatic ROI detection and extraction, eliminating trivial data, and thereby reducing the size of an underwater image. This results in drastic reduction in processing time as shown in fig. 6 and table VIII. The storage, bandwidth, and power requirements are also reduced. Besides, the proposed algorithm efficiently dehazes underwater scene points which combats the issues involved in underwater imaging as can be understood from fig. 7 and table IV. Thus, it ensures highly accurate decision-making to avoid the undersea obstacles and hence efficient navigation of UUVs across water bodies can be achieved. Pertinent to mention here, our algorithm goes hand in hand with the UUV resource constrained network and improves its overall efficiency for adoptability in automatic undersea monitoring missions.

V. Conclusion and Future Work

UUVs have given a drastic surge to the technological uprising of underwater communication and computation. However, these vehicles involve lot of battery-powered low storage devices that demand considerable amount of power, limiting its application in undersea environment. Also, the decision-making function of these unmanned vehicles to navigate smoothly in undersea complex environment is hampered by the degraded vision. If these issues are addressed, UUV can extend not only its coverage but also pave way for real-time undersea monitoring. Therefore, keeping in view these issues, this paper proposed a light-weight algorithm enabling ocean engineers to monitor undersea life automatically and instantaneously. Our study employed an efficient DNN amalgamated with a less erroneous picture restoration scheme to solve the complex problem of underwater surveillance by performing ROI detection, extraction, and restoration, helping to dehaze a single sub-aquatic image. The proposed algorithm has experimented both YOLOV8 and YOLOV4 for degraded and diverse undersea dataset of 3000 images. The performance of both versions has been highlighted in terms of ROI detection time and accuracy. Besides, from the results obtained using SE and OE metrics, it can be concluded that our technique performed well in terms of time, resource consumption, and quality of an image compared to SOTA methods. These features validate the feasibility of this proposal for deployment in undersea environments, contributing to UUV efficiency.

The processing time of our method is less compared to SOTA algorithms; however, a requirement is felt to further decrease the computational time considering the severe resource requirements of vehicle components. Besides this, ocean engineers and researchers should also focus on developing benchmark Segment Anything Model (SAM) that can adapt to variety of downstream operations, efficient open-set recognition schemes, and efficient diffusion models for underwater image augmentation. Furthermore, we plan to include an efficient bright and red channel based dehazing scheme in our algorithm for robust prior information estimation. This can help apply this technology in other related applied domains.

References

[1] Y. Wang, D. Gu, X. Ma, J. Wang and H. Wang, “Robust real-time AUV self-localization based on stereo vision-inertia,” in IEEE Transactions on Vehicular Technology, pp. 1-11, 2023, doi:10.1109/TVT.2023.3241634

[2] A. Jamalipour, F. S. Abkenar, “Efficient task allocation protocol for a hybrid-hierarchical spatial-aerial-terrestrial edge-centric IoT architecture,” IEICE Transactions on Communications, vol. 105, no. 2, pp. 116-130, 2022

[3] F. Yu, B. He and J. -X. Liu, “Underwater targets recognition based on multiple AUVs cooperative via Recurrent Transfer-Adaptive Learning (RTAL),” in IEEE Transactions on Vehicular Technology, vol. 72, no. 2, pp. 1574-1585, 2023, doi: 10.1109/TVT.2022.3211862

[4] P. Zhu, S. Liu, T. Jiang, Y. Liu, X. Zhuang and Z. Zhang, "Autonomous reinforcement control of visual underwater vehicles: real-time experiments using computer vision," in IEEE Transactions on Vehicular Technology, vol. 71, no. 8, pp. 8237-8250, 2022, doi: 10.1109/TVT.2022.3177596

[5] S. Namasudra, P. Lorenz, and U. Ghosh, “The new era of computer network by using machine learning,” Mobile Networks and Applications, pp. 1-3, 2023, doi:10.1007/s11036-023-02114-w

[6] Z. Duo, W. Wang, H. Wang, “Oceanic mesoscale eddy detection method based on deep learning,” Remote Sensing, vol. 11, no. 16, p. 1921, 2019

[7] A. Ducournau, R. Fablet, “Deep learning for ocean remote sensing: An application of convolutional neural networks for super-resolution on satellite-derived SST data,” In 9th Workshop on Pattern Recognition in Remote Sensing, pp. 1-6, 2016, doi: 10.1109/PRRS.2016.7867019

[8] Y. Yang, J. Dong, X. Sun, E. Lima, Q. Mu, X. Wang, “A CFCC-LSTM model for sea surface temperature prediction,” IEEE Geoscience and Remote Sensing Letters, vol. 15, no. 2, pp. 207-211, 2017

[9] L. Zhang, S. Wang, “Region-of-Interest Extraction Based on Local–Global Contrast Analysis and Intra-Spectrum Information Distribution Estimation for Remote Sensing Images,” Remote Sens., 2017, vol. *9*, no. 597, 2017, doi: 10.3390/rs9060597

[10] X. Zhao, R. Tao, W. Li, W. Philips, and W. Liao, “Fractional Gabor convolutional network for multisource remote sensing data classification,” IEEE Trans. Geosci. Remote Sens., early access, Mar. 23, 2021, doi:10.1109/TGRS.2021.3065507.

[11] Y. Schechner and N. Karpel, “Recovery of underwater visibility and structure by polarization analysis,” IEEE JOE, vol. 30, no. 3, pp. 570–587, Jul. 2005

[12] Li. Yi. Chong, G. C. Ji, C. M. Run, et al., “Underwater image enhancement by dehazing with minimum information loss and histogram distribution prior, IEEE Transactions on Image Processing, vol. 25, pp. 5664-5677, 2016

[13] K. He, J. Sun, and X. Tang, “Guided image filtering,” IEEE Trans. Pattern Anal. Mach. Intell., vol. 35, no. 6, pp. 1397–1409, 2013

[14] W. Xu, S. Matzner, “Underwater fish detection using deep learning for water power applications,” International Conference on Computational Science and Computational Intelligence (CSCI), 2018, https://doi.org/10.1109/CSCI46756.2018.00067

[15] P. Drews, E. Nascimento, F. Moraes, et al, "Transmission estimation in underwater single images," in Proc. IEEE Int. Conf. Comput. Vis. Workshops, Sydney, NSW, Australia, Dec. 2013, pp. 825–830
[16] L. Chao, and M. Wang, "Removal of water scattering," In ICCET, China, 2010, vol. 2, pp. 35–39
[17] H. Y. Yang, P. Y. Chen, C. C. Huang, et al, "Low complexity underwater image enhancement based on dark channel prior," in Proc. 2nd Int. Conf. Innov. Bio-Inspired Comput. Appl., Shenzhan, China, Dec. 2011, pp. 17–20
[18] Y. T. Peng, X. Zhao, and P. C. Cosman, "Single underwater image enhancement using depth estimation based on blurriness," in Proc. IEEE Int. Conf. Image Process. (ICIP), Quebec City, QC, Canada, Sept. 2015, pp. 4952–4956
[19] X. Zhao, T. Jin, and S. Qu, "Deriving inherent optical properties from background color and underwater image enhancement,"OceanEng., vol. 94, pp. 163–172, Jan. 2015, doi:10.1016/j.oceaneng.2014.11.036
[20] N. Carlevaris-Bianco, A. Mohan, and R. M. Eustice, "Initial results in underwater single image dehazing," in Proc. MTS/IEEE SEATTLE OCEANS, vol. 27, no. 3, pp. 1–8, 2010
[21] Y. T. Peng, and P. C. Cosman, "Underwater image restoration based on image blurriness and light absorption," IEEE Trans. Image Process., vol. 26, no. 4, pp. 1579–1594, 2017
[22] W. Song, Y. Wang, D. Huang, and D. Tjondronegoro, "A rapid scene depth estimation model based on underwater light attenuation prior for underwater image restoration," in Advances in Multimedia Information Processing, 11164, pp. 678–688, 2018, doi:10.1007/978-3-030-00776-8_62
[23] J. Chiang, and Y. Chen, "Underwater image enhancement by wavelength compensation and dehazing," IEEE TIP, Vol. 21, no. 4, pp. 1756–1769, April 2012
[24] K. He, J. Sun, and X. Tang, "Single image haze removal using dark channel prior," IEEE Transactions on Pattern Analysis and Machine Intelligence, vol. 30, no. 12, pp. 2341-2353, 2011
[25] K. Panetta, "Human visual system inspired underwater image quality measures," IEEE journal of ocean engineering, 2015, doi:10.1109/JOE.2015.2469915
[26] Y. Miao, "An underwater colour image quality evaluation metric," IEEE Transactions on Image Processing, 2015, doi:10.1109/TIP.2015.2491020
[27] P. Drews, E. R. Nascimento, S. Botelho, and M. Campos, "Underwater Depth Estimation and Image Restoration Based on Single Images," in IEEE Computer Graphics and Applications, vol. 36, no. 2, pp. 24-35, March 2016
[28] J. Yuan, Z. Cai, and W. Cao, "TEBCF:Real world underwater image texture enhancement model based on blurriness and color fusion," IEEE Transactions on Geoscience and Remote Sensing, vol. 60, 2022, doi: 10.1109/TGRS.2021.3110575.
[29] N. Wang, H. Zheng, and B. Zheng, "Underwater image restoration via maximum attenuation identification," IEEE Access, vol. 5, 2017, doi: 10.1109/ACCESS.2017.2753796
[30] P-W. Pan, F. Yuan, and En Cheng, "De-scattering and edge-enhancement algorithms for underwater image restoration," Front Inform Technol Electron Eng, vol. 20, no. 6, pp. 862-871, 2019
[31] P. Zhuang and X. Ding, "Underwater image enhancement using an edge-preserving filtering retinex algorithm," Multimedia Tools and Applications, 2020, doi: 10.1007/s11042-019-08404-4
[32] G. Hou, J. Li, G. Wang, Z. Pan, and X. Zhao, "Underwater image dehazing and denoising via curvature variation regularization," Multimedia Tools and Applications, 2020, doi: 10.1007/s11042-020-08759-z
[33] A. F. M. Saifuddin Saif, "Robust underwater fish detection using an enhanced convolutional neural network," I.J. Image, Graphics and Signal Processing, vol. 3, pp. 44-54, June 2021, doi:10.5815/ijigsp.2021.03.04
[34] N. Q. Hieu, D. T. Hoang, D. Niyato, D. N. Nguyen, D. I. Kim and A. Jamalipour, "Joint power allocation and rate control for rate splitting multiple access networks with covert communications," in IEEE Transactions on Communications, doi: 10.1109/TCOMM.2023.3242670.
[35] S. Sendra, J. Lloret, J. M. Jimenez, L. Parra, "Underwater acoustic modems," IEEE Sensors Journal, vol. 16, no. 11, pp. 4063-4071, 2015.
[36] Y. Ata and K. Kiasaleh, "Analysis of optical wireless communication links in turbulent underwater channels with wide range of water parameters," in IEEE Transactions on Vehicular Technology, doi: 10.1109/TVT.2023.3235823
[37] A. Kumar and D. N. K. Jayakody, "Secure NOMA-Assisted Multi-LED underwater visible light communication," in IEEE Transactions on Vehicular Technology, vol. 71, no. 7, pp. 7769-7779, July 2022, doi: 10.1109/TVT.2022.3167992
[38] F. Zhang, C. Luo, J. Xu and Y. Luo, "An autoencoder-based i/q channel interaction enhancement method for automatic modulation recognition," in IEEE Transactions on Vehicular Technology, 2023, doi: 10.1109/TVT.2023.3248625

Sheezan Fayaz is presently pursuing the Ph.D. degree in underwater image processing from the Department of Electronics and Instrumentation Technology, University of Kashmir, India. Her current research focuses on deep learning, image processing, region of interest extraction, prior based image restoration, image enhancement, dark and bright channel techniques.

Shabir A. Parah (Member, IEEE) is currently working as a Senior Assistant Professor at the Department of Electronics and IT, University of Kashmir, Srinagar, India. His research interests include multimedia signal coding, low complexity signal processing, secure communication, digital watermarking, and steganography. He has published over 150 papers in several internationally reputed journals and conferences. He continues to figure in Stanford list of world top two percent most cited researchers in the field of AI and image processing, since 2020.

G.J Qureshi had his masters in Electronics from University of Kashmir and Ph.D. from the University of Jammu. He is presently working as the principal in degree college Hyderpora Srinagar, that falls under the jurisdiction of Higher Education Department, Government of Jammu and Kashmir, India. His research areas include image and video security, Underwater Imaging, Steganography, watermarking, multimedia authentication and optical communication. He has published more than 40 papers in journals and conferences of international repute.

Jaime Lloret (Senior Member, IEEE) is currently an Associate Professor with the Polytechnic University of Valencia. He received the B.Sc. + M.Sc. degree in physics and the B.Sc. + M.Sc. degree in electronic engineering from the University of Valencia, Valencia, Spain, in 1997 and 2003, respectively, and the Ph.D. (Dr. Ing.) degree in telecommunication engineering, Polytechnic University of Valencia, Valencia, in 2006. He is a Cisco Certified Network Professional Instructor. He worked as a network designer and the administrator in several enterprises. He has been the Chair of the Integrated Management Coastal Research Institute (IGIC) since January 2017, and he is the Head of the Active and Collaborative Techniques and Use of Technologic Resources in Education (EITACURTE) Innovation Group. Dr. Lloret is an IACM Senior Member and an IARIA Fellow.

Javier Del Ser (Senior Member, IEEE) is currently a Research Professor of Artificial Intelligence and a Leading Scientist of the OPTIMA (Optimization, Modelling, and Analytics) Research Area, TECNALIA, Basque Research and Technology Alliance, Bizkaia, Spain. He received the first Ph.D. degree (cum laude) in electrical engineering from the University of Navarra, Pamplona, Spain, in 2006, and the second Ph.D. degree (cum laude, extraordinary Ph.D. Prize) in computational intelligence from the University of Alcala, Alcala de Henares, Spain, in 2013. He is also an Adjunct Professor with the University of the Basque Country (UPV/EHU), Bilbao, Spain. He has published more than 380 scientific articles, co-supervised ten Ph.D. theses, edited seven books and coauthored nine patents. His research

interests are in the design of artificial intelligence methods for data mining and optimization applied to problems in industry, energy, mobility and health, and among others. Dr. Del Ser is a recipient of the Bizkaia Talent Prize for his research career. He is an Associate Editor of tier-one journals from areas related to Artificial Intelligence.

Khan Muhammad (Senior Member, IEEE) is currently the Director of the Visual Analytics for Knowledge Laboratory (VIS2KNOW Laboratory) and an Assistant Professor (Tenure-Track) at the Department of Applied AI, School of Convergence, College of Computing and Informatics, Sungkyunkwan University, Seoul, Republic of Korea. He received the Ph.D. degree in digital content from Sejong University, Republic of Korea, in February 2019. He worked as an Assistant Professor at the Department of Software, Sejong University, from March 2019 to February 2022. His research interests include intelligent video surveillance, medical image analysis, information security, video summarization, multimedia data analysis, computer vision, the IoT/IoMT, and smart cities. He has registered ten patents and published over 230 papers in peer-reviewed journals and conference proceedings in his research areas. He is an associate editor or an editorial board member of more than 14 journals. According to the Web of Science/Clarivate, he is among the most highly cited researchers, in 2021 and 2022.